HHS Public Access

Author manuscript

Nanomedicine. Author manuscript; available in PMC 2023 February 01.

Published in final edited form as:

Nanomedicine. 2022 February ; 40: 102483. doi:10.1016/j.nano.2021.102483.

Cerium oxide nanoparticle conjugation to microRNA-146a mechanism of correction for impaired diabetic wound healing

Lindel C. Dewberry[1], **Stephen M. Niemiec**[1], **Sarah A. Hilton**[1], **Amanda E. Louiselle**[1], **Sushant Singh**[2,3], **Tamil S. Sakthivel**[2], **Junyi Hu**[1], **Sudipta Seal**[2], **Kenneth W. Liechty**[1], **Carlos Zgheib**[1]

[1]Laboratory for Fetal and Regenerative Biology, Department of Surgery, University of Colorado Denver School of Medicine and Children's Hospital Colorado, Aurora, CO

[2]Department of Materials Science and Engineering, Advance Materials Processing Analysis Center, Nanoscience Technology Center, University of Central Florida, Orlando, FL

[3]Amity Institute of Biotechnology, Amity University Chhattisgarh, Raipur-493225, Chhattisgarh, India

Abstract

Diabetic wounds represent a significant healthcare burden and are characterized by impaired wound healing due to increased oxidative stress and persistent inflammation. We have shown that CNP-miR146a synthesized by the conjugation of cerium oxide nanoparticles (CNP) to microRNA (miR)-146a, improves diabetic wound healing. CNP are divalent metal oxides that act as free radical scavenger, while miR146a inhibits the pro-inflammatory NFκB pathway, so CNP-miR146a has a synergistic role in modulating both oxidative stress and inflammation. In this study, we define the mechanism(s) by which CNP-miR146a improves diabetic wound healing by examining immunohistochemical and gene expression analysis of markers of inflammation, oxidative stress, fibrosis, and angiogenesis. We have found that intradermal injection of CNP-miR146a increases

[*]**Corresponding Author:** Carlos Zgheib, PhD, Assistant Professor of Surgery, University of Colorado Denver-Anschutz Medical Campus, Barbara Davis Center for Childhood Diabetes, 1775 Aurora Ct, M20-3305, Aurora, CO 80045, Phone: (303) 724-3041, Carlos.Zgheib@CUAnschutz.edu.

Credit Author Statement

Lindel C. Dewberry: Conceptualization, data curation, formal analysis, investigation, methodology, project administration, visualization, roles/writing – original draft, writing – review & editing.
Stephen M. Niemiec: Conceptualization, formal analysis, methodology, project administration, visualization, roles/writing – original draft, writing – review & editing.
Sarah A. Hilton: Conceptualization, data curation, formal analysis, investigation, methodology, project administration, visualization, roles/writing – original draft, writing – review & editing.
Amanda E. Louiselle: Investigation, methodology, project administration, writing – review & editing.
Sushant Singh: Data curation, investigation, methodology, project administration, resources, writing – review & editing.
Tamil S Sakthivel: Data curation, investigation, methodology, project administration, resources, writing – review & editing.
Junyi Hu: Data curation, investigation, methodology, project administration, resources, writing – review & editing.
Sudipta Seal: Conceptualization, funding acquisition, project administration, supervision, validation, writing – review & editing.
Kenneth W. Liechty: Conceptualization, funding acquisition, project administration, supervision, validation, writing – review & editing.
Carlos Zgheib: Conceptualization, funding acquisition, project administration, supervision, validation, writing – review & editing.

wound collagen, enhances angiogenesis, and lowers inflammation and oxidative stress, ultimately promoting faster closure of diabetic wounds.

Graphical Abstract

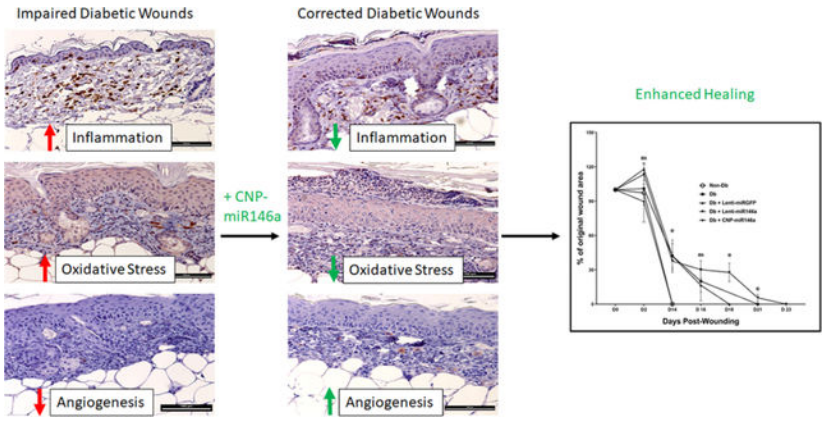

Diabetic wounds are characterized by increased inflammation and oxidative stress, which results in impaired angiogenesis and delayed wound healing. CNP-miR146a, the conjugation of ROS scavenging cerium oxide nanoparticles (CNP) to anti-inflammatory microRNA (miR)-146a, synergistically lowers inflammation and oxidative stress, improving histologic evidence of angiogenesis and collagen deposition, and ultimately accelerating wound closure.

Keywords

Diabetic wounds; cerium oxide nanoparticle (CNP); CNP-miR146a; inflammation; angiogenesis; oxidative stress

Introduction:

The number of people diagnosed with diabetes has significantly increased since the 1980s with a prevalence now exceeding 400 million individuals worldwide (1). As the incidence of diabetes continues to rise, the associated comorbidities and healthcare costs have escalated as well. Diabetic wounds, specifically lower extremity ulcers, represent a significant healthcare burden with the cost of care for lower extremity ulcers ranging from $9 to $13 billion annually (2).

We have previously shown that diabetic skin has impaired biomechanical properties compared to normal skin (3). This weakened skin, along with diabetic neuropathy and vasculopathy, predispose diabetic patients to wounds and ulcers. Normal wound healing is an ordered process that proceeds through the distinct phases of inflammation, proliferation, and remodeling (4). However, diabetic wounds are characterized by increased levels of oxidative stress and persistent inflammation, leading to increased risk of chronic wound formation (5). Macrophages, fibroblasts, and endothelial cells produce proinflammatory cytokines such as interleukin (IL)-6, which in turn recruit additional inflammatory cells to the injured tissue, perpetuating the inflammatory cycle. This is further amplified in

diabetic wounds through high levels of reactive oxygen species which simultaneously activate proinflammatory transcription factors such as Nuclear Factor Kappa B (NFκB) (6, 7). Therefore, targeting oxidative stress and inflammatory pathways provides a potential therapeutic avenue to alter the wound microenvironment toward a more homeostatic state.

A recent surge in research has demonstrated that microRNAs (miRNA, miR), small non-coding RNA molecules, have regulatory functions in wound healing and are often dysregulated in diabetic wounds (8–14). One miRNA in particular, miRNA-146a (miR146a), targets the NFκB pathway by downregulating IL-1 receptor-associated kinase (IRAK1) and tumor necrosis factor (TNF) receptor associated factor 6 (TRAF6) (15). MiR146a inhibition of IRAK1 and TRAF6 downregulates NFκB activity, which ultimately leads to decreased expression of pro-inflammatory cytokines like IL-6 and IL-8 (16). We have previously shown that miRNA-146a levels are significantly reduced in diabetic wounds compared to non-diabetic wounds, so increasing miRNA-146a levels could reduce inflammatory signaling and correct healing (12). MiRNA-146a may also improve wound healing through modulation of vascular endothelial growth factor (VEGF) and B cell lymphoma (BCL)-2 expression, which are both active by hypoxia-inducible factor (HIF) 1-α, although its effects on angiogenesis in diabetic wounds is still under investigation. VEGF plays an important role in diabetic wound healing by promoting angiogenesis, increasing oxygen delivery to wounds, and inducing BCL-2 to prevent endothelial cell apoptosis (17, 18).

One challenge with using small nucleic acids as unmodified therapeutics is they have rapid pharmacokinetics, can be degraded quickly, and carry a highly negative charge that may reduce cellular uptake (19, 20). Nanotechnology allows for novel delivery methods to stabilize miRNA molecules. In recent years, we and others have studied the potential of cerium oxide nanoparticles (CNPs) to be used as an antioxidative based drug delivery system (21–24). CNPs have a Ce^{+3} redox active state and Ce^{+4} oxidation state, which can act as a free radical scavenger. The Ce^{+4} oxidation state is covered by the presence and absence of oxygen vacancies formed during the cerium oxide nanoparticle crystal lattice synthesis. The oxygen vacancies create the catalytic hotspots for its different chemical and biochemical redox reactions (25, 26). These highly antioxidative CNPs have been used for their in vitro and in vivo reactive oxygen species (ROS) scavenging properties and found to be highly effective in modulating oxidative stress (23, 27). All together, these CNPs' properties have made them a lucrative material for further numerous biotherapeutic applications.

We have developed a novel strategy to synergistically target both inflammation and oxidative stress in diabetic wounds by designing and synthesizing CNPs conjugated to a miR146a mimetic to target both the inflammatory response and oxidative stress in diabetic wounds (28). We have shown that this conjugate, CNP-miR146a, accelerates diabetic wound healing in two animal models of impaired diabetic wound healing: a diabetic mouse model and a diabetic porcine model (28, 29). However, the underlying mechanism(s) of this correction remain(s) to be determined. Given the antioxidative and anti-inflammatory properties of the conjugate components, we hypothesize that CNP-miR146a improves diabetic wound healing by synergistically targeting the pro-inflammatory NFκB signaling pathway and decreasing

oxidative stress, thus creating a wound microenvironment conducive for angiogenesis, collagen deposition, and healing.

Methods:

CNP-miR146a Conjugate Synthesis

CNPs were synthesized using the previously published approach of simple wet chemistry (30). In detail, stoichiometric amount of cerium nitrate hexahydrate (purity level 99.999%) was added to ultrapure water and mixed homogenously. Excess hydrogen peroxide (H_2O_2) was added as an oxidizer to the cerium solution and the pH was maintained below 4 to produce CNPs. These ultra-small CNPs were used further for miR146a conjugation using 1,1-carbonyldiimidazole (CDI) chemistry using earlier published protocol (28) (Figure S1A). In this approach carbonyldiimidazole leads to formation of an intermediate imidazole group compound which is highly sensitive to reaction with the free amine group of the miRNA leading to formation of amine bonds. Thus, here the free amine group added to the 3'end of the miR146a molecules reacts to from the amine bond leading to the surface conjugation of the molecules onto the CNPs employed. The conjugate is dialyzed in DNAse/RNAse free water and stored in −20°C in different volume aliquots until further use. The oxidation process leads to the development of the crystalline CNPs which were characterized for their size and surface charge using Zeta Sizer Nano (Malvern Instruments). Characterization of zeta surface charge and sizing comparing CNP and CNP-miR146a has been recently published (29).

CNP-miR146a Characterization with Infrared and X-ray Photoelectron Spectroscopy

Fourier-transform infrared (FTIR) spectroscopy measurements were performed to analyze the different conjugating parameters. Antioxidative superoxide dismutase (SOD) enzyme mimetic property were evaluated using the Sigma Aldrich 19160 KTF assay kit (31). X-ray photoelectron spectroscopic (XPS) analysis was also performed in detail to understand any change in the CNP chemical structure and its conjugation chemistry. X-ray photoelectron spectroscopy (XPS) was carried out using Thermo fisher ESCALAB 250xi spectrometer with a monochromatic Al Kα x-ray source. The calibration of the binding energy in the spectral lines was carried out referring to the C1s emission line (284.6eV). The core level peak fitting was performed by using a Smart background and mixed Lorentzian–Gaussian. The deconvolution has been performed to further verify every unresolved peak. FTIR analysis was employed to verify this conjugation chemistry. The presence of amide region peaks in the range of 1600 and 1340–1385 indicated the successful conjugation among the products. The XPS measurement was also performed to find the chemical composition of miRNA before and after conjugation, as well as the valence state of CeO_2 nanoparticles. Ce3d envelops are recorded to find the chemical conjugation regarding the valence state of CNPs, where a peak around 915 eV correlates to a Ce^{+4} oxidation state and will reduce upon conjugation with miR146a, denoting a change in the nanoceria matrix. Results are described in Supporting Information, Figure S1B,C.

SOD Activity of CNP and CNP-miR146a

To further evaluate the role of CNP-miR146A in reducing oxidative stress, an antioxidative SOD enzyme mimetics assay was performed. Antioxidative SOD enzyme mimetic property were evaluated using Sigma Aldrich 19160 KTF assay kit for CNP and CNP-miR146a, and compared to kit controls (31). Results are described in Supporting Information, Figure S2.

In Vitro Assessment of CNP-miR146a Delivery of miR-146a

CNP-miR-146a was designed to improve delivery of miR-146a to the wound, thereby restoring the healing capacity. To examine the ability of exogenously administered CNP-miR-146a to increase the level of miR-146a in fibroblasts *in vitro*, murine non-diabetic (1×10^6 cells) or diabetic (1×10^6 cells) fibroblasts were incubated in culture with PBS, 0.1 ng of CNP, or 0.1 ng of CNP-miR-146a for 24 hours. Following incubation, total cellular RNA was isolated from the cells by homogenizing in Qiazol (Qiagen) per manufacturer instructions. Isolated RNA was converted to U6 and miR-146a cDNA (Applied Biosystems RT kit), where U6 is the housekeeper gene used for normalization. cDNA was amplified with BioRad CFX-9600 thermal cycler and U6 and miR-146a levels were quantified in triplicate by real-time quantitative polymerase chain reaction (RT-qPCR). Average relative expression of miR-146a compared to U6 for each triplicate was used for normalization and compared across groups. Results are described in Supporting Information, Figure S3.

Animals

All experimental protocols were approved by the Institutional Animal Care and Use Committee at University of Colorado Denver - Anschutz Medical Campus and followed the guidelines described in the NIH Guide for the Care and Use of Laboratory Animals. For experiments, 12-week-old female mice homozygous for the $Lepr^{db}$ mutation (db/db) and age-matched female nondiabetic heterozygous littermates (db/+) were used (BKS.Cg-$Dock^{7m+/+}Lepr^{db}$/J, strain No. 000642, Jackson Laboratory).

Diabetic Murine Wound Healing Model

Mice were anesthetized with inhaled isoflurane during wounding. Each mouse was shaved and depilated on their dorsal aspect, and the dorsal skin was swabbed with alcohol and Betadine (Purdue Pharma). Each mouse underwent a single dorsal full-thickness wound (including panniculus carnosus) with an 8-mm punch biopsy (Miltex Inc). These wounds were treated by intradermal injection with 50 ul of PBS, 10^6 PFU LentimiR-146a, 10^6 PFU Lenti-GFP-Control miR, or 1 ng CNP-miR146a at the time of wounding. The PBS treated group represented the baseline diabetic control group, while lenti-miR146a is a miR146a mimetic to act as a therapeutic control and lenti-miRGFP (Control miR) is a scrambled miRNA that acts as an additional non-therapeutic control. We previously tested CNP treatment alone and we found that it did not improve diabetic wound healing, and therefore CNP injections were not repeated in this study to reduce animal and resource waste (29, 32). All wounds were dressed with Tegaderm (3M), which was subsequently removed on postoperative day 2. Postoperatively, the mice received a subcutaneous injection of an analgesic, buprenorphine (Schering-Plough Animal Health Corp).

Measurement of Wound Size Over Time

Wound photographs were obtained every other day including a ruler for measurement in each image until wounds were fully closed (n = 5 per group). ImageJ software (National Institutes of Health; http://rsbweb.nih.gov/ij/) was then used to calculate the wound area. A blinded observer analyzed the size of each wound. Wound area as a percentage of original wound size was plotted as a function of time for statistical comparison between groups.

Creation and Treatment of Murine Wounds for Mechanism Studies

Because we found CNP-miR146a, rather than the above controls, was the only group to return diabetic wound healing to a non-diabetic phenotype (Figure 1), we evaluated only the PBS and CNP-miR146a treatments for the remaining mechanistic studies in both diabetic and non-diabetic mice. An 8mm dorsal wound was performed on age-matched diabetic and non-diabetic mice, as described above. Diabetic and non-diabetic mice were treated at the time of wounding with intradermal injection of CNP-miR146a, as above, or an equivalent volume of PBS as a control. Wounds for mechanistic studies were harvested at seven days post-wounding.

Histology and Immunohistochemistry Analysis

The mice (n = 5 per group) had wounds harvested at seven days and placed in 10% formalin solution for 24 hours prior to histologic processing. Tissue was dehydrated in 70% ethanol prior to embedding, and five-micron sections were taken from embedded tissue and placed on positive charged slides. A subset of slides for each sample underwent Masson's Trichrome or Hematoxylin and Eosin (H&E) staining. Masson's Trichrome stain was used for collagen quantification, while H&E stain was used to image the thickness of the dermis and epidermis. Using NIS Elements – Advanced Research imaging software, five 100x total magnification images (10x objective lens) were taken along the wound edge to capture the entire tissue section. A second, blinded observer then measured the area of blue stain, or collagen area, per high power field (HPF) for collagen quantification.

The remaining slides were used for immunohistochemistry. Antigen retrieval was performed using 13 Antigen Retrieval Citra (BioGenex HK086-9k, Fremont, CA) in a decloaking chamber using the factory default settings (Biocare Medical, Concard, CA). Slides were rinsed three times in 0.1% Triton100 in PBS (PBST) and blocked in 20% goat serum in 0.4% PBST for 60 min at room temperature. This was followed by overnight incubation at room temperature with primary antibodies against cluster of differentiation (CD) 45 (rabbit polyclonal ab10558, 1:100; Abcam, Cambridge, MA) in 5% goat serum and 0.1% PBST, CD 31, or NADPH oxidase 2 (NOX2). The following day, slides were washed three times in 0.1% PBST and incubated with the appropriate anti-rabbit biotinylated secondary antibodies for 1 h at room temperature. Slides were washed three times in 0.1% PBST and mounted in Vectashield (Vector Laboratories, Burlingame, CA). The slides were then incubated with avidin-biotin-peroxidase complex (Vector Laboratory) and developed, as described by the manufacturer. CD45 is a common leukocyte antigen that stains white blood cells within the tissue sample for quantification. CD 31, also known as platelet endothelial cell adhesion molecule (PECAM-1), is a protein present on endothelial cells and can be used to quantify the number of blood vessels per HPF. NOX2, also known as cytochrome b(558)

subunit beta, is an enzyme that generates super-oxides and can be quantified to evaluate ROS-producing cells. For each stain, 200x total magnification images were taken along the wound edge. Number of positive-stained cells (cell count) per HPF was then quantified by a second experimenter as described above.

Analysis of Pro-inflammatory and Pro-angiogenic Gene Signaling

Wounded skin was collected at seven days. Tissue was processed for total RNA extraction as described above to convert to cDNA. For miRNA quantification, miR-146a was again compared to U6 as a housekeeper gene. For mRNA quantification, 18s was used as the housekeeper gene for normalization. RT-qPCR was performed for miR-146a, U6, 18s, IRAK1, TRAF6, NFκB, IL-6, VEGF, Bcl-2, and HIF1-α. Samples (n= 5 per group) were amplified in triplicate and results were averaged for each.

Statistical Analysis

Results are expressed as mean ± SEM. Statistical significance involving single comparisons was determined by a Student's t test. For multiple comparisons, ANOVA followed by an appropriate post hoc test as noted was performed (Fisher's LSD post-hoc test). A $p<0.05$ was taken as significant. All statistics were performed using Graphpad Prism Software (LaJolla, CA).

Results:

CNP-miR146a Accelerates Diabetic Wound Healing

In this time to full wound closure experiment, our data show that diabetic wounds treated with CNP-miR146a demonstrated significantly improved healing ($p<0.05$), reaching wound closure at the same time as the non-diabetic group (Day 14 post-wounding). These diabetic wounds treated with CNP-miR146a reached wound closure faster compared to those treated with PBS, lenti-miRGFP, or lenti-miR146a (Figure 1).

CNP-miR146a Normalizes Inflammation in Diabetic Wounds

Figure 2A–D shows the relative gene expression of pro-inflammatory genes IRAK1, TRAF6, NFκB, and IL-6. Examining IRAK1 and TRAF6 gene expression at day 7 post wounding, PBS treated diabetic wounds had significantly higher levels of both IRAK1 and TRAF6 gene expression compared to PBS treated non diabetic wounds ($p<0.05$). Expression of IRAK1 and TRAF6 significantly decreased ($p<0.05$) with treatment of CNP-miR146a in the diabetic wounds (Figure 2A, B). Gene expression of NFκB and IL-6 at day 7 post wounding were also significantly higher in PBS treated diabetic wounds (Db-CTL) compared to PBS treated non-diabetic wounds (NDb-CTL) ($p<0.05$), but CNP-miR146a returned these to control non-diabetic levels (Figure 2C, D; $p<0.05$).

When comparing non-diabetic and diabetic wounds at day 7 post wounding, PBS treated diabetic wounds had decreased levels of miR146a gene expression ($p<0.05$). This significantly improved after treatment with CNP-miR146a ($p<0.05$), nearly reaching non diabetic levels of miR146a (Figure 2E).

We performed immunohistochemistry analysis for CD45, the common leukocyte antigen that is present on all inflammatory cells. The number of CD45+ cells was quantified per HPF and averaged for each sample. Representative images for each group are depicted in Figure 2F. Our data showed that diabetic control wounds had significantly more CD45+ cells/HPF ($p<0.01$) compared to non-diabetic control wounds ($p<0.05$) (Figure 2G). In contrast, diabetic wounds treated with CNP-miR146a demonstrated a significant reduction in the number of CD45+ inflammatory cells, reducing CD45+ numbers to a similar level to non-diabetic wounds ($p<0.05$).

CNP-miR146a Decreases Oxidative Stress in Diabetic Wounds

Immunohistochemistry staining of wound sections for NOX2, a well-known producer of ROS and marker of oxidative stress, was performed for samples collected seven days after wounding. Representative images of each group are shown in Figure 3A. Immunohistochemistry demonstrated increased numbers of NOX2+ cells in diabetic wounds compared to non-diabetic wounds ($p<0.05$). After treatment with CNP-miR146a, there was a significant decrease in the number of NOX2+ cells in diabetic wounds ($p<0.005$) (Figure 3B).

CNP-miR146a Increases Angiogenesis in Diabetic Wounds

Using RT-qPCR, we analyzed the relative expression levels of pro-angiogenic factors VEGF, Bcl-2, and HIF1-α in diabetic and non-diabetic wounds treated with PBS or CNP-miR146a. Our data show that PBS-treated diabetic wounds demonstrated decreased gene expression of VEGF and BCL2 compared to non-diabetic wounds ($p<0.05$) and CNP-miR146a significantly increased these levels at 7 days post-treatment ($p<0.05$) (Figure 4A and B). In addition, we looked at the expression of Hypoxia Induced Factor 1 alpha (HIF-1a), a transcription factor known to induce the expression of VEGFa and BCL2. Our data show that CNP-miR146a significantly increased these levels at 7 days post-treatment ($p<0.05$) (Figure 4C).

We used CD31 immunohistochemistry staining to evaluate the formation of blood vessels, as depicted in Figure 4D. We found significantly decreased numbers of CD31+ cells in diabetic wounds compared to non-diabetic wounds. Treatment with CNP-miR146a increased the numbers of CD31+ cells in diabetic wounds compared to PBS treated diabetic wounds ($p<0.05$) (Figure 4E).

CNP-miR146a Increases Collagen Deposition in Diabetic Wounds

Representative images of trichrome staining are depicted in Figure 5A. Trichrome staining showed a decreased collagen deposition in diabetic wounds compared to non-diabetic wounds (Figure 5B, $p<0.05$). However, these levels were increased after treatment with CNP-miR146a in diabetic wounds ($p<0.01$). Representative images of H&E staining in Figure 5C demonstrate a thicker dermal and epidermal layer in diabetic wounds treated with CNP-miR146a compared to PBS treatment.

Discussion:

In this study, we show that CNP-miR146a acts by decreasing inflammation and oxidative stress, increasing angiogenesis, and improving collagen deposition to accelerate diabetic wound healing.

Nanoparticles have been used to deliver miRNA therapeutics to treat a number of different diseases and disorders(33). A recent publication has also shown that virus-like particles can act as carrier for miR-146a delivery and suppress the production of auto-antibodies in lupus-prone mice(34), however, the use of nanoparticles to deliver miRNA to correct the diabetic wound healing impairment has not been investigated until recently (28). One of the many advantages of CNPs over current systems used to deliver miRNA, is that CNPs are potent inhibitors of oxidative stress due to their ROS scavenging ability, similar to the enzymatic activity of superoxide dismutase (SOD) and catalase (35), and are not toxic in vivo (36). This study demonstrates that CNP conjugation to miR-146a can be done with CDI chemistry to maintain the ROS scavenging activity of CNP while successfully delivering miR-146a to the target tissue. We also see that even after successful conjugation to miR-146a, CNP maintains Ce^{3+} redox activity regions and reduces oxidative stress (Figure S2). Our choice of CNPs is based on the advantages of CNPs over other nanomaterials that have been used for gene delivery: 1) CNPs have an auto-regenerative surface, so small amounts function in ROS scavenging for a long time(37); 2) CNPs also possess anti-bacterial properties(38); 3) CNPs can directly shuttle miR-146a directly into the cytoplasm without sub-cellular targeting and will increase the life-time of miRNA-146a attached to the CNPs (39).

The dual role of targeting the inflammatory response with miR-146a delivery and decreasing oxidative stress via the CNP's ROS scavenging properties represents a novel and promising treatment to correct the diabetic wound healing impairment. MiRNAs play an important role in the various phases of wound healing and have been studied for their therapeutic potential in wound healing (40, 41). We saw no improvement in wound healing with miR146a administration alone. This may be secondary to the delivery of miRNAs in general being limited by the challenging nature of miRNA stability and their tendency to degradation, and CNP can act not only as a vehicle for miR-146a delivery but as a therapeutic component as well.

Our data show that treatment of diabetic murine wounds with CNP-miR146a results in improved wound healing with a shorter time to wound closure. This improved wound healing is facilitated through correcting the expression of miR146a in diabetic wounds, which results in decreased expression of TRAF6, IRAK1, ultimately leading to decreased expression of NFKB and IL-6. Pro-inflammatory cytokines activate recruited macrophages to produce further IL-6, IL-1β, and TNFα, sustaining an inflammatory wound microenvironment. This decrease in inflammation and oxidative stress was further supported with reduced number of CD45+ and NOX2+ cells on immunohistochemistry in wounds treated with CNP-miR146a. CD45 is a common leukocyte antigen, so we are unable to differentiate if these are neutrophils or macrophages, however, both cell populations are known to contribute to increased inflammation and ROS and future investigation of cell

specific effects, like macrophage polarity, will help further elucidate the improvements seen in diabetic wound healing with CNP-miR146a (42).

CNP-miR146a treatment was associated with an increase in expression of VEGF and Bcl-2, suggesting the reduced inflammation and oxidative stress early in the wound healing process may create a suitable microenvironment for angiogenesis. MiR146a has been previously implicated in enhancing angiogenic activity in endothelial cells (43, 44). IL-6, TNFα, and other pro-inflammatory cytokines like IL-1β inhibit VEGF signaling pathways, lowering angiogenesis and fibroblast recruitment (42). Fibroblasts play an important role in ECM remodeling following resolution of inflammation, and increased levels of pro-inflammatory cytokines in diabetic wounds has been shown to inhibit myofibroblast activity, contributing to chronic wound formation (42, 45). Wound treated with CNP-miR146a demonstrated improved wound architecture, both with greater dermal thickness and higher collagen deposition. Fibroblast activity may be modulated by the less inflammatory microenvironment within the wound, as recruited CD45+ cells within the wound bed produce recalcitrant inflammation through ongoing IL-6 and TNFα production. We know that miR146a levels increase in fibroblasts cultured with CNP-miR146a, and wound fibroblasts play a critical role in cellular migration and wound remodeling. This is supported by other studies which have demonstrated the role of various miRNAs, including miR-146a, in changing the extracellular matrix composition by targeting fibronectin and fibroblast activity (46).

Diabetic wounds are a significant healthcare problem with high associated costs of care. Therefore, the development of a novel therapeutic that improves wound healing has the potential to considerably impact this disease. The reduced time to wound closure that is noted with CNP-miR146a administration has implications in regard to reduced healthcare costs not only due to reduced wound care time but also preventing the progression of a wound to the point that amputation is necessary. This study expands upon our previous work with CNP-miR146a in diabetic wound healing, and is the first to evaluate the maintained redox potential of CNP after conjugation to miR146a and investigate the effect of CNP-miR146a on NOX-2 expression, while also examining the gene expression profile of the NFκB inflammatory pathway in the wound after treatment with CNP-miR146a.

In conclusion, CNP-miR146a improves wound healing by reducing inflammation and oxidative stress by targeting the NFκB pathway and lowering oxidative stress. This reduction promotes a wound microenvironment conducive to angiogenesis as well as collagen deposition, further correcting the impairment in diabetic wound healing.

Supplementary Material

Refer to Web version on PubMed Central for supplementary material.

Acknowledgements:

The authors would like to acknowledge and thank the University of Colorado Denver Histology Resource Center for their contribution to this work.

Conflicts of Interest and Source of Funding: Supported by funds from NIH R01 DK118793 01A1 to Kenneth W. Liechty, MD and the University of Colorado Denver and Children Hospital Colorado. The University of Central Florida (UCF) collaborators acknowledges the funding from NSF MRI XPS: ECCS:1726636 for XPS measurement.

References:

1. Emerging Risk Factors C, Sarwar N, Gao P, Seshasai SR, Gobin R, Kaptoge S, et al. Diabetes mellitus, fasting blood glucose concentration, and risk of vascular disease: a collaborative meta-analysis of 102 prospective studies. Lancet. 2010;375(9733):2215–22. [PubMed: 20609967]
2. Rice JB, Desai U, Cummings AK, Birnbaum HG, Skornicki M, Parsons NB. Burden of diabetic foot ulcers for medicare and private insurers. Diabetes Care. 2014;37(3):651–8. [PubMed: 24186882]
3. Bermudez DM, Herdrich BJ, Xu J, Lind R, Beason DP, Mitchell ME, et al. Impaired biomechanical properties of diabetic skin implications in pathogenesis of diabetic wound complications. Am J Pathol. 2011;178(5):2215–23. [PubMed: 21514435]
4. Lepantalo M, Apelqvist J, Setacci C, Ricco JB, de Donato G, Becker F, et al. Chapter V: Diabetic foot. Eur J Vasc Endovasc Surg. 2011;42 Suppl 2:S60–74. [PubMed: 22172474]
5. Falanga V Wound healing and its impairment in the diabetic foot. Lancet. 2005;366(9498):1736–43. [PubMed: 16291068]
6. Zgheib C, Hodges MM, Hu J, Liechty KW, Xu J. Long non-coding RNA Lethe regulates hyperglycemia-induced reactive oxygen species production in macrophages. PLoS One. 2017;12(5):e0177453. [PubMed: 28494015]
7. Wei W, Liu Q, Tan Y, Liu L, Li X, Cai L. Oxidative stress, diabetes, and diabetic complications. Hemoglobin. 2009;33(5):370–7. [PubMed: 19821780]
8. Berger AG, Chou JJ, Hammond PT. Approaches to Modulate the Chronic Wound Environment Using Localized Nucleic Acid Delivery. Adv Wound Care (New Rochelle). 2020.
9. Pishavar E, Behravan J. miR-126 as a Therapeutic Agent for Diabetes Mellitus. Curr Pharm Des. 2017;23(22):3309–14. [PubMed: 28440196]
10. Sekar D, Venugopal B, Sekar P, Ramalingam K. Role of microRNA 21 in diabetes and associated/related diseases. Gene. 2016;582(1):14–8. [PubMed: 26826461]
11. Wu Y, Zhang K, Liu R, Zhang H, Chen D, Yu S, et al. MicroRNA-21–3p accelerates diabetic wound healing in mice by downregulating SPRY1. Aging (Albany NY). 2020;12(15):15436–45. [PubMed: 32634115]
12. Xu J, Wu W, Zhang L, Dorset-Martin W, Morris MW, Mitchell ME, et al. The role of microRNA-146a in the pathogenesis of the diabetic wound-healing impairment: correction with mesenchymal stem cell treatment. Diabetes. 2012;61(11):2906–12. [PubMed: 22851573]
13. Zgheib C, Liechty KW. Shedding light on miR-26a: Another key regulator of angiogenesis in diabetic wound healing. J Mol Cell Cardiol. 2016;92:203–5. [PubMed: 26906635]
14. Zhang Y, Sun X, Icli B, Feinberg MW. Emerging Roles for MicroRNAs in Diabetic Microvascular Disease: Novel Targets for Therapy. Endocr Rev. 2017;38(2):145–68. [PubMed: 28323921]
15. Taganov KD, Boldin MP, Chang KJ, Baltimore D. NF-kappaB-dependent induction of microRNA miR-146, an inhibitor targeted to signaling proteins of innate immune responses. Proc Natl Acad Sci U S A. 2006;103(33):12481–6. [PubMed: 16885212]
16. Bhaumik D, Scott GK, Schokrpur S, Patil CK, Orjalo AV, Rodier F, et al. MicroRNAs miR-146a/b negatively modulate the senescence-associated inflammatory mediators IL-6 and IL-8. Aging (Albany NY). 2009;1(4):402–11. [PubMed: 20148189]
17. Xu XW, Zhang J, Guo ZW, Song MM, Sun R, Jin XY, et al. A narrative review of research progress on the relationship between hypoxia-inducible factor-2alpha and wound angiogenesis. Ann Palliat Med 2021;10(4):4882–8. [PubMed: 33966427]
18. Zubair M, Ahmad J. Role of growth factors and cytokines in diabetic foot ulcer healing: A detailed review. Rev Endocr Metab Disord. 2019;20(2):207–17. [PubMed: 30937614]
19. Dowdy SF. Overcoming cellular barriers for RNA therapeutics. Nat Biotechnol. 2017;35(3):222–9. [PubMed: 28244992]

20. Johannes L, Lucchino M. Current Challenges in Delivery and Cytosolic Translocation of Therapeutic RNAs. Nucleic Acid Ther. 2018;28(3):178–93. [PubMed: 29883296]
21. Sack M, Alili L, Karaman E, Das S, Gupta A, Seal S, et al. Combination of conventional chemotherapeutics with redox-active cerium oxide nanoparticles--a novel aspect in cancer therapy. Mol Cancer Ther. 2014;13(7):1740–9. [PubMed: 24825856]
22. Eitan E, Hutchison ER, Greig NH, Tweedie D, Celik H, Ghosh S, et al. Combination therapy with lenalidomide and nanoceria ameliorates CNS autoimmunity. Exp Neurol. 2015;273:151–60. [PubMed: 26277686]
23. Dowding JM, Song W, Bossy K, Karakoti A, Kumar A, Kim A, et al. Cerium oxide nanoparticles protect against Abeta-induced mitochondrial fragmentation and neuronal cell death. Cell Death Differ. 2014;21(10):1622–32. [PubMed: 24902900]
24. Deshpande S, Patil S, Kuchibhatla SV, Seal S. Size dependency variation in lattice parameter and valency states in nanocrystalline cerium oxide. Applied Physics Letters. 2005;87(13):133113.
25. Kumar A, Babu S, Karakoti AS, Schulte A, Seal S. Luminescence properties of europium-doped cerium oxide nanoparticles: role of vacancy and oxidation states. Langmuir. 2009;25(18):10998–1007. [PubMed: 19735149]
26. Korsvik C, Patil S, Seal S, Self WT. Superoxide dismutase mimetic properties exhibited by vacancy engineered ceria nanoparticles. Chem Commun (Camb). 2007(10):1056–8. [PubMed: 17325804]
27. Chigurupati S, Mughal MR, Okun E, Das S, Kumar A, McCaffery M, et al. Effects of cerium oxide nanoparticles on the growth of keratinocytes, fibroblasts and vascular endothelial cells in cutaneous wound healing. Biomaterials. 2013;34(9):2194–201. [PubMed: 23266256]
28. Zgheib C, Hilton SA, Dewberry LC, Hodges MM, Ghatak S, Xu J, et al. Use of Cerium Oxide Nanoparticles Conjugated with MicroRNA-146a to Correct the Diabetic Wound Healing Impairment. Journal of the American College of Surgeons. 2019;228(1):107–15. [PubMed: 30359833]
29. Niemiec SM, Louiselle AE, Hilton SA, Dewberry LC, Zhang L, Azeltine M, et al. Nanosilk Increases the Strength of Diabetic Skin and Delivers CNP-miR146a to Improve Wound Healing. Front Immunol 2020;11:590285. [PubMed: 33193424]
30. Karakoti AS, Monteiro-Riviere NA, Aggarwal R, Davis JP, Narayan RJ, Self WT, et al. Nanoceria as Antioxidant: Synthesis and Biomedical Applications. JOM (1989). 2008;60(3):33–7. [PubMed: 20617106]
31. Singh S, Ly A, Das S, Sakthivel TS, Barkam S, Seal S. Cerium oxide nanoparticles at the nano-bio interface: size-dependent cellular uptake. Artificial Cells, Nanomedicine, and Biotechnology. 2018;46(sup3):S956–S63.
32. Zgheib C, Hilton SA, Dewberry LC, Hodges MM, Ghatak S, Xu J, et al. Use of Cerium Oxide Nanoparticles Conjugated with MicroRNA-146a to Correct the Diabetic Wound Healing Impairment. J Am Coll Surg. 2019;228(1):107–15. [PubMed: 30359833]
33. Zhang Y, Satterlee A, Huang L. In vivo gene delivery by nonviral vectors: overcoming hurdles? Mol Ther. 2012;20(7):1298–304. [PubMed: 22525514]
34. Pan Y, Jia T, Zhang Y, Zhang K, Zhang R, Li J, et al. MS2 VLP-based delivery of microRNA-146a inhibits autoantibody production in lupus-prone mice. Int J Nanomedicine. 2012;7:5957–67. [PubMed: 23233803]
35. Asati A, Santra S, Kaittanis C, Perez JM. Surface-charge-dependent cell localization and cytotoxicity of cerium oxide nanoparticles. ACS Nano. 2010;4(9):5321–31. [PubMed: 20690607]
36. Cai X, Seal S, McGinnis JF. Non-toxic retention of nanoceria in murine eyes. Mol Vis. 2016;22:1176–87. [PubMed: 27746672]
37. Das S, Dowding JM, Klump KE, McGinnis JF, Self W, Seal S. Cerium oxide nanoparticles: applications and prospects in nanomedicine. Nanomedicine (Lond). 2013;8(9):1483–508. [PubMed: 23987111]
38. Shah V, Shah S, Shah H, Rispoli FJ, McDonnell KT, Workeneh S, et al. Antibacterial activity of polymer coated cerium oxide nanoparticles. PLoS One. 2012;7(10):e47827. [PubMed: 23110109]

39. Singh S, Ly A, Das S, Sakthivel TS, Barkam S, Seal S. Cerium oxide nanoparticles at the nano-bio interface: size-dependent cellular uptake. Artif Cells Nanomed Biotechnol. 2018;46(sup3):S956–S63. [PubMed: 30314412]
40. Banerjee J, Chan YC, Sen CK. MicroRNAs in skin and wound healing. Physiol Genomics. 2011;43(10):543–56. [PubMed: 20959495]
41. Li D, Landen NX. MicroRNAs in skin wound healing. Eur J Dermatol. 2017;27(S1):12–4. [PubMed: 28690209]
42. Cooper PO, Haas MR, Noonepalle SKR, Shook BA. Dermal Drivers of Injury-Induced Inflammation: Contribution of Adipocytes and Fibroblasts. Int J Mol Sci. 2021;22(4).
43. Zhu K, Pan Q, Zhang X, Kong LQ, Fan J, Dai Z, et al. MiR-146a enhances angiogenic activity of endothelial cells in hepatocellular carcinoma by promoting PDGFRA expression. Carcinogenesis. 2013;34(9):2071–9. [PubMed: 23671131]
44. Li Y, Zhu H, Wei X, Li H, Yu Z, Zhang H, et al. LPS induces HUVEC angiogenesis in vitro through miR-146a-mediated TGF-beta1 inhibition. Am J Transl Res. 2017;9(2):591–600. [PubMed: 28337286]
45. Goldberg MT, Han YP, Yan C, Shaw MC, Garner WL. TNF-alpha suppresses alpha-smooth muscle actin expression in human dermal fibroblasts: an implication for abnormal wound healing. J Invest Dermatol. 2007;127(11):2645–55. [PubMed: 17554369]
46. Feng B, Chen S, McArthur K, Wu Y, Sen S, Ding Q, et al. miR-146a-Mediated extracellular matrix protein production in chronic diabetes complications. Diabetes. 2011;60(11):2975–84. [PubMed: 21885871]

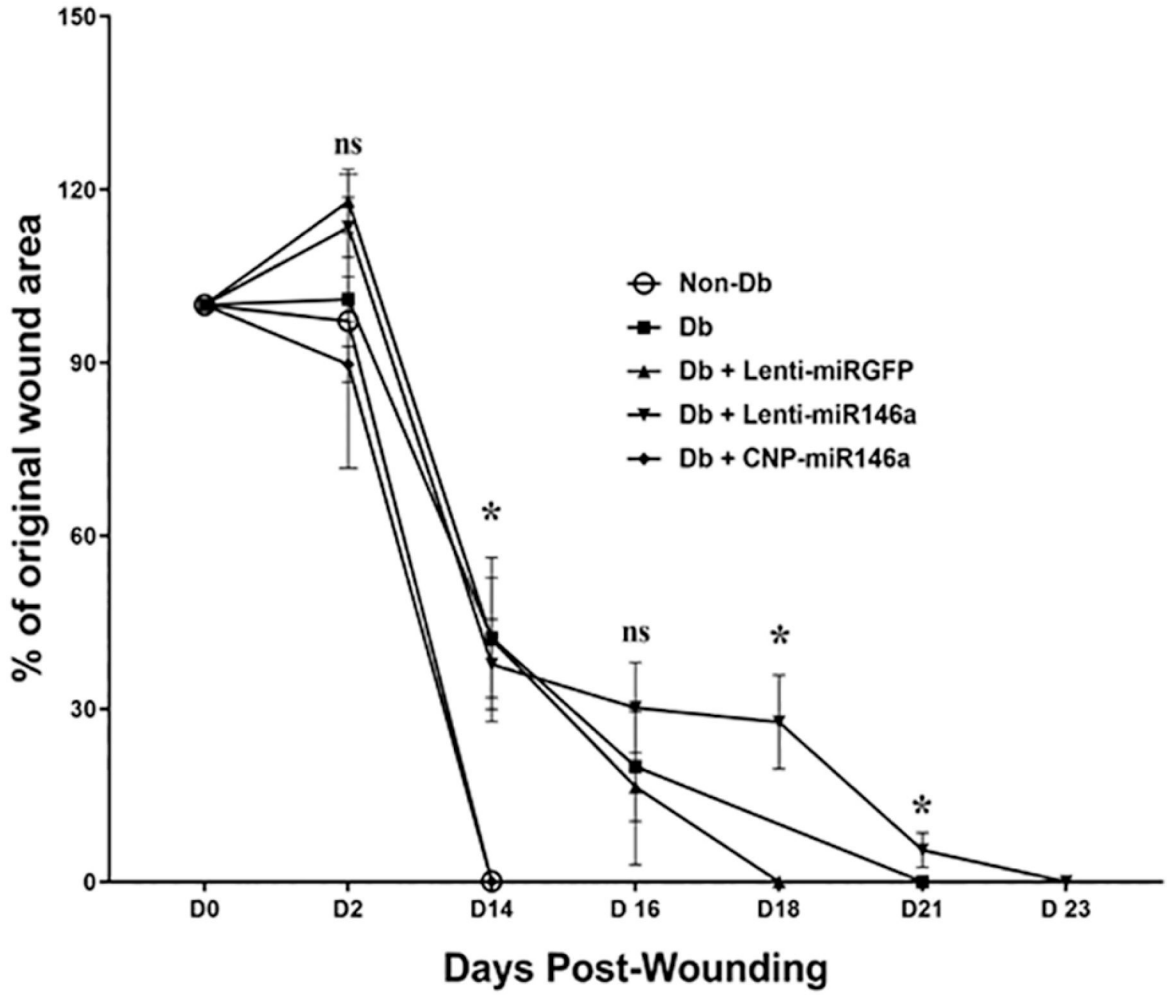

Figure 1:

Wound closure over time.

Analysis comparing the percent of the original wound area by group is depicted for each time point. Non-diabetic wounds were compared to untreated diabetic wounds, and diabetic wounds treated with lenti-miRGFP, lenti-miR146a, or CNP-miR146a. Wounds treated with CNP-miR146a demonstrated significantly improved wound healing ($p<0.05$) and had the same time to wound closure as non-diabetic wounds (day 14). At day 14, the non-diabetic group and the Db CNP-miR146a group has significantly less wound area than the remaining diabetic groups. At day 18, the Db Lenti-miR146a group was significantly more open than the Db Lenti-miRGFP group. At day 21, the Db Lenti-miR146a group has significantly more wound area than the diabetic group alone. *Indicates $p < 0.05$.

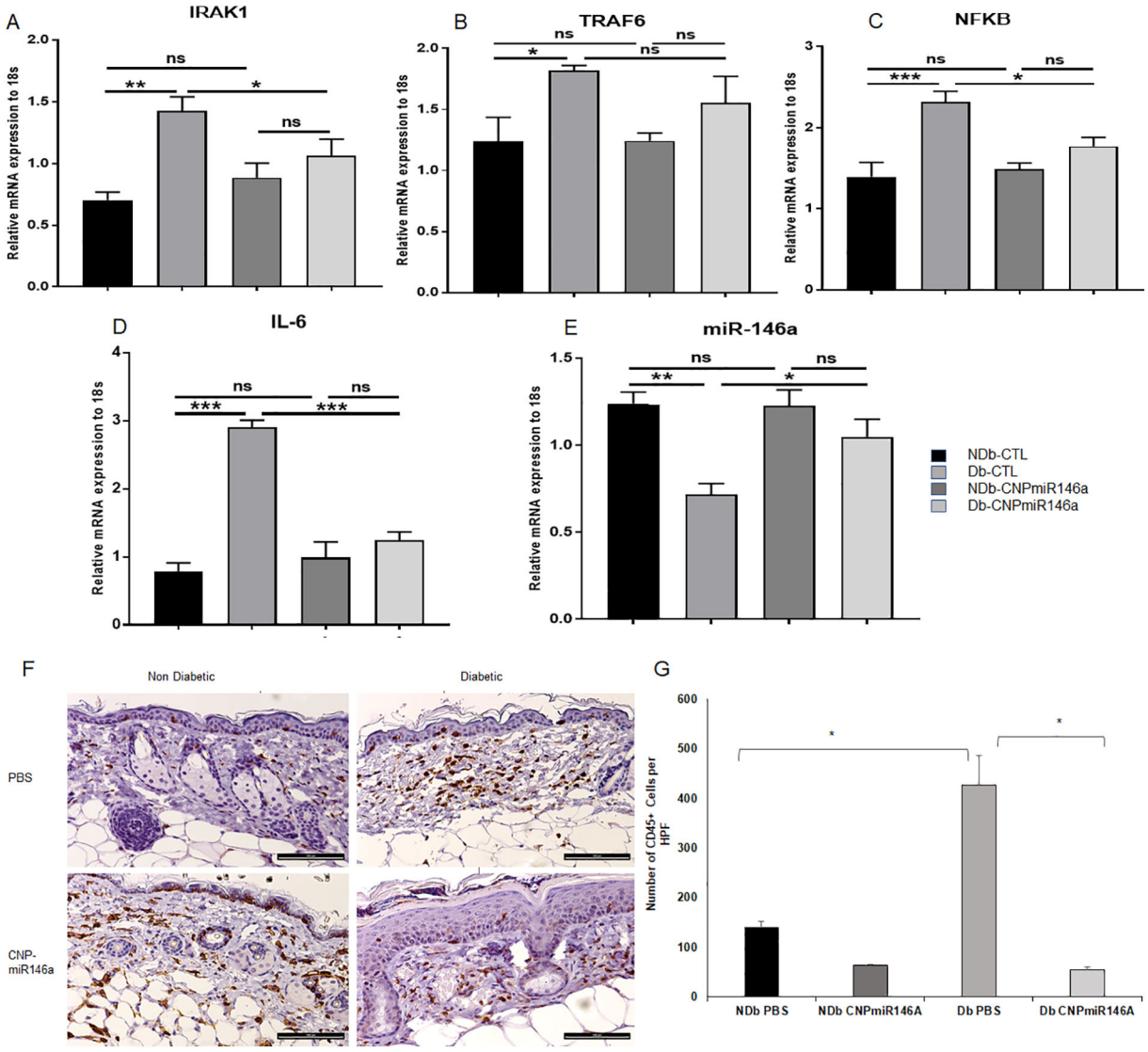

Figure 2:

Inflammation and Inflammatory Cell Infiltrate are Decreased with CNP-miR146a treatment in Diabetic Wounds.

(A) Gene Expression Day 7 Post Wounding. IRAK1 levels decreased in diabetic wounds after treatment with CNP-miR146a ($p<0.05$) (B) TRAF6 levels decreased in diabetic wounds after treatment with CNP-miR146a ($p<0.05$) (C) NFκB levels decreased in diabetic wounds after treatment with CNP-miR146A ($p<0.05$) (D) IL-6 levels decreased in diabetic wounds after treatment with CNPmiR146A ($p<0.05$) (E) miR146a levels increased in diabetic wounds after treatment with CNPmiR146a ($p<0.05$). (F) CD45+ Staining in Day 7 Non-diabetic and Diabetic Wounds with and without CNP-miR146a treatment (bar represents 100μm). (G) Diabetic wounds treated with CNPmiR146a demonstrated decreased staining of CD45+ cells per HPF (*p = 0.01). NDb-CTL = non-diabetic, untreated control; Db-CTL = diabetic, untreated control; NDb-CNP-miR146a = non-diabetic, CNP-miR146a treated; Db-CNPmiR146a = diabetic, CNP-miR146a treated.

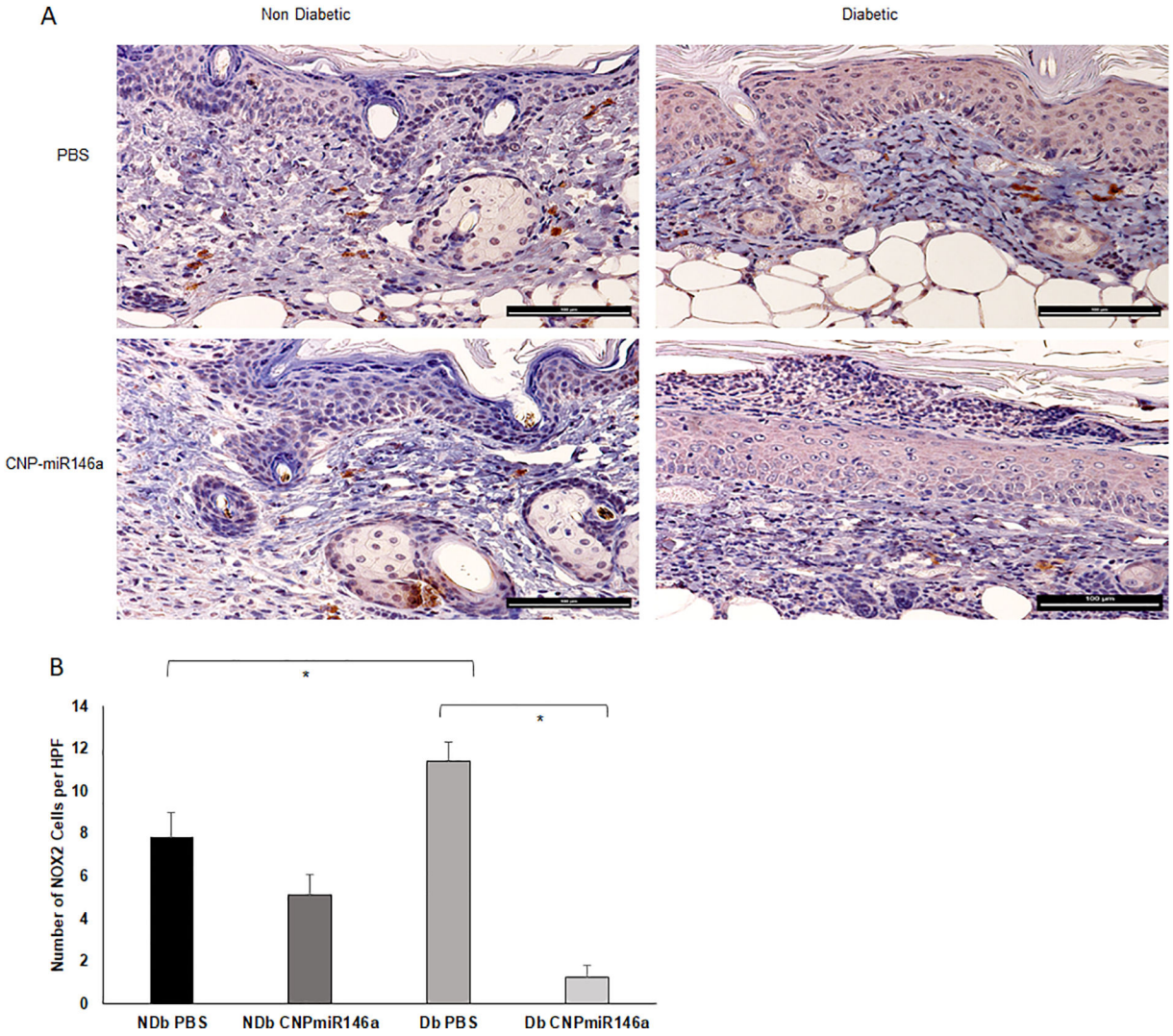

Figure 3:

Modulation of NOX2+ Expression with CNP-miR146a

(A) NOX2+ Staining in Day 7 Non-diabetic and Diabetic Wounds (bar represents 100μm). (B) At day 7 after wounding, immunohistochemistry demonstrated increases numbers of NOX2+ cells in diabetic wounds compared to non-diabetic wounds ($p=0.02$). After treatment with CNP-miR146a, there was a significant decrease in the number of NOX2+ cells in diabetic wounds ($p<0.005$). *Indicates $p<0.05$.

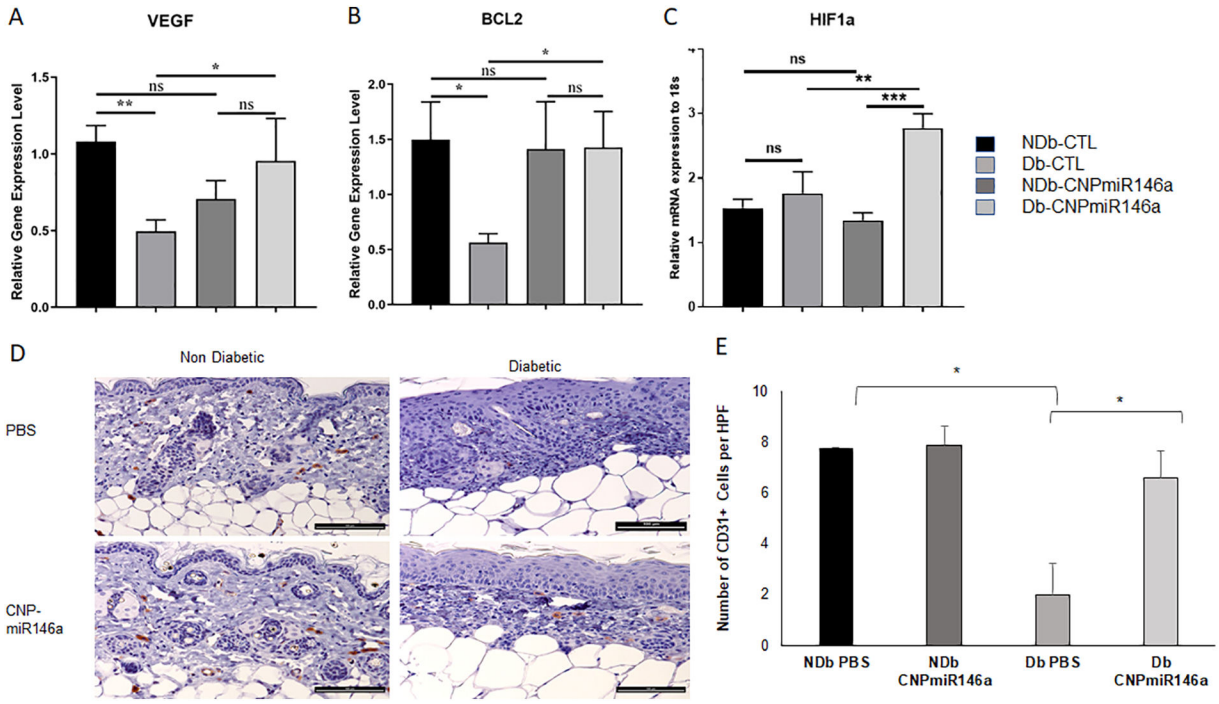

Figure 4:

Pro-Angiogenic Gene Expression Day 7 Post Wounding.

(A-C) Diabetic wounds demonstrated increased gene expression of VEGF, BCL2, and HIF1a when treated with CNP-miR146a ($p<0.05$). (D) Representative images of CD31+ staining in day 7 non-diabetic and diabetic wounds (bar represents 100μm). (E) Diabetic wounds treated with CNPmiR146a demonstrated increased staining of CD31+ cells ($p<0.05$).

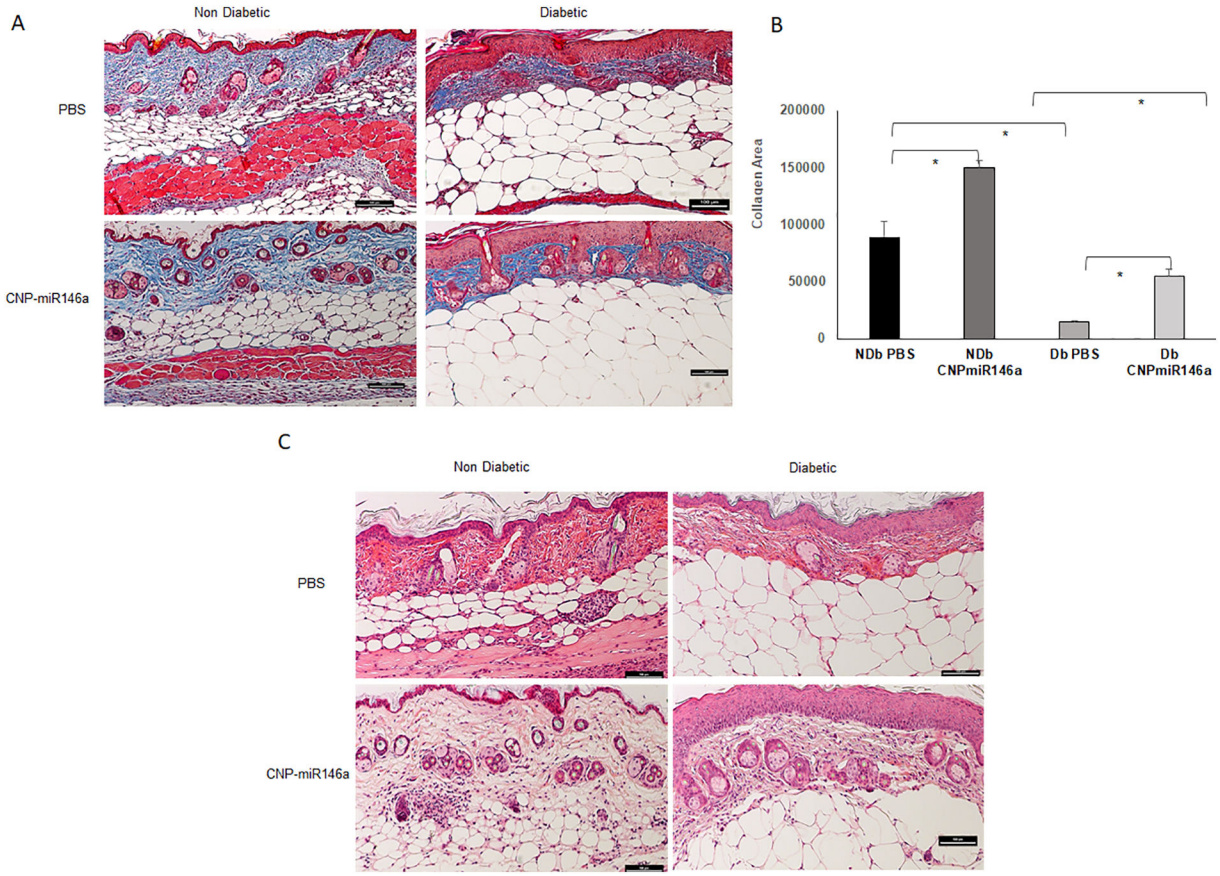

Figure 5:

ECM Remodeling Changes with CNP-miR146a

(A) Trichrome (collagen) staining of day 7 diabetic wounds (bar represents 100μm). (B) At day 7 after wounding, histochemistry demonstrated a decreased area of collagen (blue staining) in diabetic wounds compared to non-diabetic wounds ($p<0.05$). After treatment with CNP-miR146a, there was a significant increase in the area of collagen (blue staining) in diabetic wounds ($p<0.01$). (C) Representative images of H&E staining showing increased dermal and epidermal thickness in diabetic wounds after treatment with CNP-miR146a.